Case Studies in Thermal Engineering 66 (2025) 105770

Contents lists available at ScienceDirect

Case Studies in Thermal Engineering

journal homepage: www.elsevier.com/locate/csite

Experimental case study for optimizing heat sink performance using ZnO nanocarriers integrated with phase change materials for environmental sustainability

Muhammad Farooq [a,*], Imran Zahid [b,**], M. Yasar Javaid [b], Noreen Sher Akbar [a], Enio Pedone Bandarra Filho [a], M. Farrukh Shahzad [c], M. Imran Khan [a], Mohammad Ilyas Khan [d], Mohammad Rehan [e], Fahid Riaz [f]

[a] Department of Mechanical Engineering, College of Engineering, Prince Mohammad Bin Fahd University, Al-Khobar, Saudi Arabia
[b] Department of Mechanical Engineering and Technology, Government College University Faisalabad, Pakistan
[c] College of Economics and Management, Beijing University of Technology, Beijing, China
[d] Department of Chemical Engineering, College of Engineering, King Khalid University, Abha, Saudi Arabia
[e] Center of Excellence in Environmental Studies (CEES), King Abdulaziz University, Jeddah, Saudi Arabia
[f] Department of Mechanical Engineering, Abu Dhabi University, Abu Dhabi, United Arab Emirates

ARTICLE INFO

Keywords:
Copper foam
RT-54HC (PCM)
Clean energy storage solution
Zero emission thermal management
ZnO nanocarriers

ABSTRACT

Electronic equipment generates heat during prolonged operation, making efficient heat dissipation essential to ensure continuous functionality and prevent premature device failure. Accordingly, phase change materials (PCMs) were employed for thermal management; however, their low thermal conductivity limits their effectiveness in temperature-sensitive electronic systems. PCMs can be made more thermally conductive with the use of nanocarriers-based phase change materials (NcPCMs), which could lower system temperatures and increase device operational lifetimes. In this study, the main objective is to improve overall performance of heat sinks by integrating ZnO nanocarriers into RT54HC (PCM) to enhance thermal conductivity using ZnO/RT54HC (NcPCM) across various transient heat energy loads (09 W–27 W) and different optimal saturation levels of ZnO, varying between 1.0 wt% to 3.0 wt%. Simple and copper foam embedded heat sinks demonstrated significant temperature reduction by incorporating ZnO into cooling media within the internal cavities in contrast to the unfilled, unfinned heat sink under all heat inputs. These findings showed the effectiveness of NcPCM based copper sink in reducing peak temperature of 24.02 % and improving operational time of 35 and 69 min at targeted critical temperatures of 50 °C and 60 °C owing to favorable characteristics of high thermal conductivity and increased surface area. Hence, the incorporation of nanocarriers into nontoxic environment friendly PCMs is strongly advocated to promote sustainable progress in electronic thermal management, as it offers clean, zero-emission energy storage solution.

* Corresponding author.
** Corresponding author.
E-mail addresses: engrfarooq137@gmail.com (M. Farooq), imranzahid@gcuf.edu.pk (I. Zahid).

https://doi.org/10.1016/j.csite.2025.105770
Received 23 September 2024; Received in revised form 16 December 2024; Accepted 7 January 2025
Available online 9 January 2025

1. Introduction

Effective thermal management (TM) is essential to ensure the durability and optimal performance of electronic components [1–3]. This necessity arises from the swift progression of technological advancements, continual efforts in miniaturization, elevated data processing speeds and increasing power demands, which cause overheating problems [4–7]. TM, or controlling the heat, is crucial for this reason. Inadequate control of temperature might lead to early device malfunctions [8–10]. A study reveals that 55 % of electronics malfunction because of overheating and temperature exceeding operational limits [11]. Consequently, quick heat dispersion from electrical circuits is necessary to improve the cooling efficiency of electronic equipment [12].

Advances in cooling methods have been the subject of numerous research, including spray cooling, air cooling, forced air cooling, two-phase (liquid-vapor) cooling, nanofluid-based liquid cooling, and jet impingement cooling [13–16]. However, these technologies involve rotating components like fans and pumps that contribute to weight and complexity, increasing costs and operational disruptions due to maintenance needs [17–20]. It is therefore possible that active cooling methods are impractical for small electronic devices.

Phase change materials (PCMs), with their large thermal energy storage capacity, are frequently used with passively cooled heat sinks [21–23]. Because of their promising qualities, including high latent and specific heat, reusability, minimal supercooling, a broad melting and solidifying temperature range, chemical stability, and non-corrosive behavior, organic PCMs are favored for TM applications [12,24–26]. However, the primary concern with PCM is restricted heat transfer to the surroundings, attributed to their limited thermal conductivity [27,28]. Various techniques are proposed to counter the thermal conductivity challenge as shown in Fig. 1.

Nedumaran et al. [34] studied numerically and experimentally pin fin heat sinks with n-eicosane as a PCM under varying heating conditions. The variation in pin height accelerated melting rate. The triangular-finned heat sink exhibited a faster melting and solidification rate compared to other pin-fin heat sinks. The increase in heating power shortens the base temperature. Tharwan and Hadidi [35] experimentally investigated on solid and hollow rectangular plate fins with and without PCM. Their work presented a phase-transition material integrated into a heat sink that controls the temperature of electronics, especially useful for controlling thermal shock. Elshaer et al. [36] used RT35, organic PCM, to regulate the thermal conditions of the small satellite subsystems. Six different pin fin geometries with 20 % and 50 % volume fractions were employed for experimental purposes. The result indicated a significant reduction of 5.7 °C in the base plate temperature of thermal control equipment as the number of square fins increased from 15 to 80.

A comparative investigation was studied by Talele and Zhao [37] for battery TM using PCM and nano-PCM. Al_2O_3-PCM outer performed conventional paraffin wax PCM in delaying battery maximum temperature due to its superior heat transmission, preventing premature liquefaction. Bhutto et al. [38] studied various types of nanocarriers with PCM for passive cooling system. The goal of keeping the battery's maximum surface temperature below 50 °C and its ΔTmax below 5 °C was achieved. Moaveni et al. [39] studied hybrid and passive TM system using PCM, nano-PCM, fins and metallic foam. Findings revealed that including 9 % nanocarriers and 4 fins in the hybrid mode reduces peak temperature by 5.18 K and 10.36 K, respectively, compared to hybrid modes lacking fins and nanocarriers.

The literature presented in Table 1 indicates a growing preference for PCM/NcPCM-based heat sink in recent years for TM of electronics. However, many studies have primarily examined the impact of heat sink geometry with PCM, with only a limited number investigating metallic foams and with nanocarriers PCM-based heat sink. The present study conducted an experimental investigation to explore the effects of RT54HC (PCM) and ZnO nanocarriers on simple and metallic foam-based heat sink performance. Nanocarriers phase change material (NcPCM), specifically (ZnO/PCM), with varying concentrations of nanocarriers (ranging from 1.0 wt% to 3.0 wt %), is incorporated into simple and foam-based heat sinks. The integration of ZnO nanocarriers in organic PCMs within heat sinks represents a promising advancement in thermal management for environmental sustainability. Organic PCMs, including paraffin (RT54HC) and fatty acids, are frequently sourced from sustainable/biodegradable or renewable materials, rendering them more environmentally sustainable than synthetic options. By using ZnO nanocarriers, abled to enhance the thermal properties, which

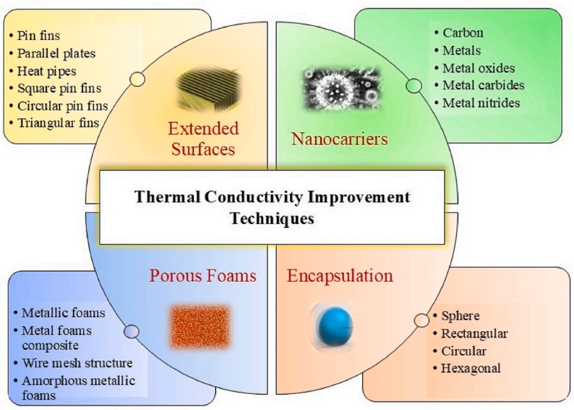

Fig. 1. Various thermal conductivity improvement methods of PCMs [29–33].

Table 1
Summary of nanocomposites with PCMs used in various thermal management systems.

Sr. No	PCM and Melting Temperature (°C)	Nanocarriers (wt.%)	Heat Sink/Geometry (mm^3)	Power (W)/ Temperature (°C)	Applications	Authors
1	RT-27 (27–28)	–	108 × 30 × 65 (Rectangular Cube)	–	Battery Thermal management	[40]
2	RT-54 HC (52–54)	–	100 × 100 × 25	8, 16 & 24	Electronics cooling	[41]
3	PT-58 (58)	Silica, Carbon black (0.25 & 0.5)	–	–	PV Module	[42]
4	Paraffin wax (25)	Graphene, Silver (0.1, 0.3 & 0.5)	–	–	Building thermal comfort	[43]
5	Paraffin wax (40–47)	Silicon carbide (1,2 & 3)	50 × 50 × 5	15, 20, 35 & 45	Electronic Components	[44]
6	RT-42	MWCNT (3 & 6)	110 × 110 × 25	10	Electronic Devices	[45]
7	RT-82	SWCNT, Graphene (1,2,3)	Double tube Pipe (fins)	–	Heat Exchanger	[46]
8	RT-70HC RT-54HC	Al_2O_3 (0.15, 0.20 & 0.25)	100 × 100 × 27 (Square fins)	10, 20 & 30	Thermal Energy Storage	[47–50]
9	Lauric acid (41–44.2)	Al_2O_3 and CuO (0.1)	Shell and tube	–	Engine waste recovery	[51]

allowed for more efficient heat dissipation using less material and less resource usage overall. Compared to other nanocarriers based on metals or carbon, ZnO nanocarriers have a smaller environmental impact due to their abundance and lack of toxicity. The utilization of active cooling systems is lessened, leading to lower energy consumption and carbon gas emissions, due to combination of ZnO and PCM. This setup aims to analyze the heat transfer performance under different input powers, with the objective of enhancing the operational efficiency of electronic devices across different set point temperatures.

2. Experimental setup

Fig. 2 illustrates the schematic representation of the current experimental setup which comprises a DC power unit, heat sink geometry for thermal management, data recorder and workstation. The rubber electrical heater, situated at the base of the heat sink assembly, generated heat energy by a dc supply. 9–27 W of heating output might be produced by varying the voltage of a DC power source. The heat produced by the heater simulates the thermal output generated by the processor/chip during operation. To minimize the air entrapment and lower thermal resistance between the heater and heat sink base, the heater was affixed to the bottom cavity using specialized thermal adhesive. A thermal adhesive (Vkingkeyn, China) with a thermal conductivity of 1.96 W/m·K was used to bond the silicon plate heater to the back groove of the heat sink. Its low thickness (<0.1 mm) effectively prevents the accumulation of trapped air, and the minimal layer thickness ensures negligible thermal resistance.

2.1. *Composite heat sink assembly*

An aluminum heat sink, featuring internal dimensions of 100 × 100 × 32 mm^3, is preferred over copper-based heat sink. This preference is attributed to its excellent thermal conductivity, low coefficient of thermal expansion, lightweight nature, lower density, corrosion resistance and high thermal diffusion. These qualities collectively make it a suitable and advantageous option for thermal inspection purposes. Insulation is applied to the four side walls of the sink, while its top is covered with copper plate to enable one dimensional heat flow from the heat sink.

The composite section of this heat sink comprises both metal foam and ZnO/PCM. The metal foam of similar dimension of internal cavity of heat sink having thermal conductivity 395 W/mK and porosity of 93 % was tested into heat sink. Prior to its utilization in thermal analysis within the heat sink, it undergoes cleaning with water and acetone. The design detail of the heat sinks being examined thermally are illustrated in Fig. 3.

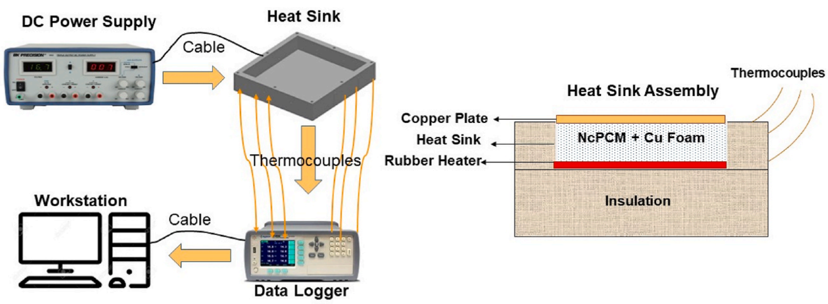

Fig. 2. Experimental setup for thermal management of NcPCM-based heat sink.

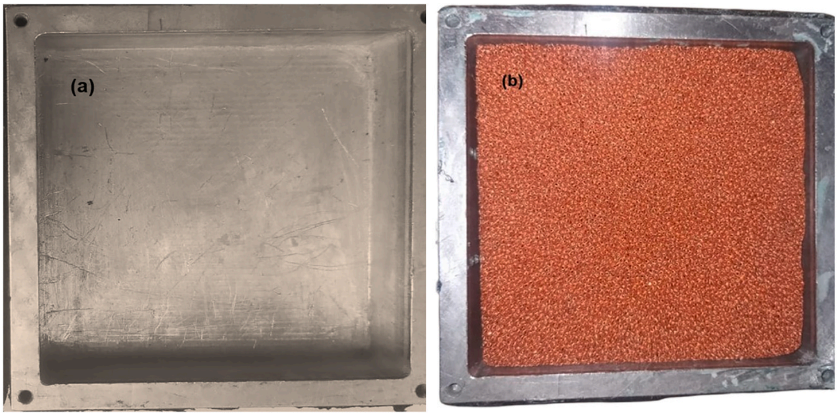

Fig. 3. Simple and copper foam-based heat sinks.

2.2. NcPCM preparation

The selection of PCM, particularly RT54HC and ZnO-nanocarriers was made considering their thermos-physical properties with the aim of enhancing thermal conductance of the heat sink as shown in Table 2.

ZnO nanocarriers were the preferred choice for their unique nanostructure characteristics, high thermal conductivity, effective dispersion stability and cost-effectiveness for enhancing thermal conductivity of RT54HC, PCM. The SEM image accompanied by energy dispersive X-ray (EDX) analysis of ZnO nanocarriers, which provides information about the morphology and elemental composition are depicted in Fig. 4(a and b). The size distribution of non-spherical shape nanocarriers was analyzed using Image J software, as depicted in Fig. 4(c), revealing an average size of approximately 0.43 μm. Initially, crystalline solid, PCM, was preheated to its designated melting point temperature to its liquid state. Subsequently, to create NcPCM blend, varying concentrations of ZnO nanocarriers were introduced into a molten cooling medium. The resulting mixture was magnetically stirred consistently for uniform dispersion of nano carriers, and the temperature was kept at 40 °C, above the liquification temperature of the PCM. Following this, the blend underwent ultrasonication for 2 h before being utilized as the final mixture. The ultrasonication not only improved the solubility of nanocarriers in liquid cooling media but also helped in removing agglomeration and preparing a homogeneous mixture [52,53]. The method of synthesis is depicted in Fig. 5 below. The above NcPCM preparing method was repeated for 1 wt%, 2 wt%, 3 % wt.%, 4 wt% and 5 wt% of ZnO nano carriers into PCM. %. The addition of ZnO from 1 wt% to 3 wt% significantly enhanced the thermal conductivity of the PCM. However, at 4 wt% of ZnO nanocarriers, the thermal conductivity plateaued, and further increasing the concentration to 5 wt% resulted in a decline. Therefore, the samples with the highest thermal conductivity (1 wt% to 3 wt%) were selected and introduced into the heat sink cavity to achieve optimal thermal management performance. Following this, the sample was introduced into the heat sink, and the stability of the prepared samples was assessed visually. Quality control checks of the PCM were examined after each test, revealing no indication of sedimentation.

3. Validation and uncertainty analysis of experimental design

Before analyzing the results, experimental setup was endorsed through a comparative assessment of an empty heat sink against previous studies conducted by Leong et al. [54] and Tariq et al. [55]. The temperature trend observed aligns with that of the empty heat sink in this study, ranging from 28 °C to 54 °C. A heat sink with inner dimensions of 102 × 102 × 27 mm and a heating input are utilized to establish a correlation between the results. Fig. 6 illustrates a close agreement between current study and previous research. The slight deviation of 6–7 % in the temperature profile can be attributed to variances in heating power and ambient conditions. Consequently, further investigation is underway to evaluate the effectiveness of the heat sink under different scenarios.

Uncertainty in experimentation arises from either instrument imprecision or human error. After analysis, it's important to quickly detect and eliminate erroneous data to ensure the authenticity of the results. Kline and McClintock [56] devised a root-sum-square combination method to estimate uncertainty in experimental parameters. This approach involves expressing a variable as Equation (2).

$$Z = m_{easured} \pm \delta z \tag{2}$$

Table 2
Properties of PCM and nanocarriers.

Material	Melting Point (°C)	Specific heat (KJ/Kg.K)	Density (Kg/m^3)	Purity	Thermal conductivity	Latent Heat (kJ/kg)
RT54HC	53–54	2	0.8 (l), 0.85 (s)	–	0.2	200
ZnO	1975	–	5606	100	2.5	–

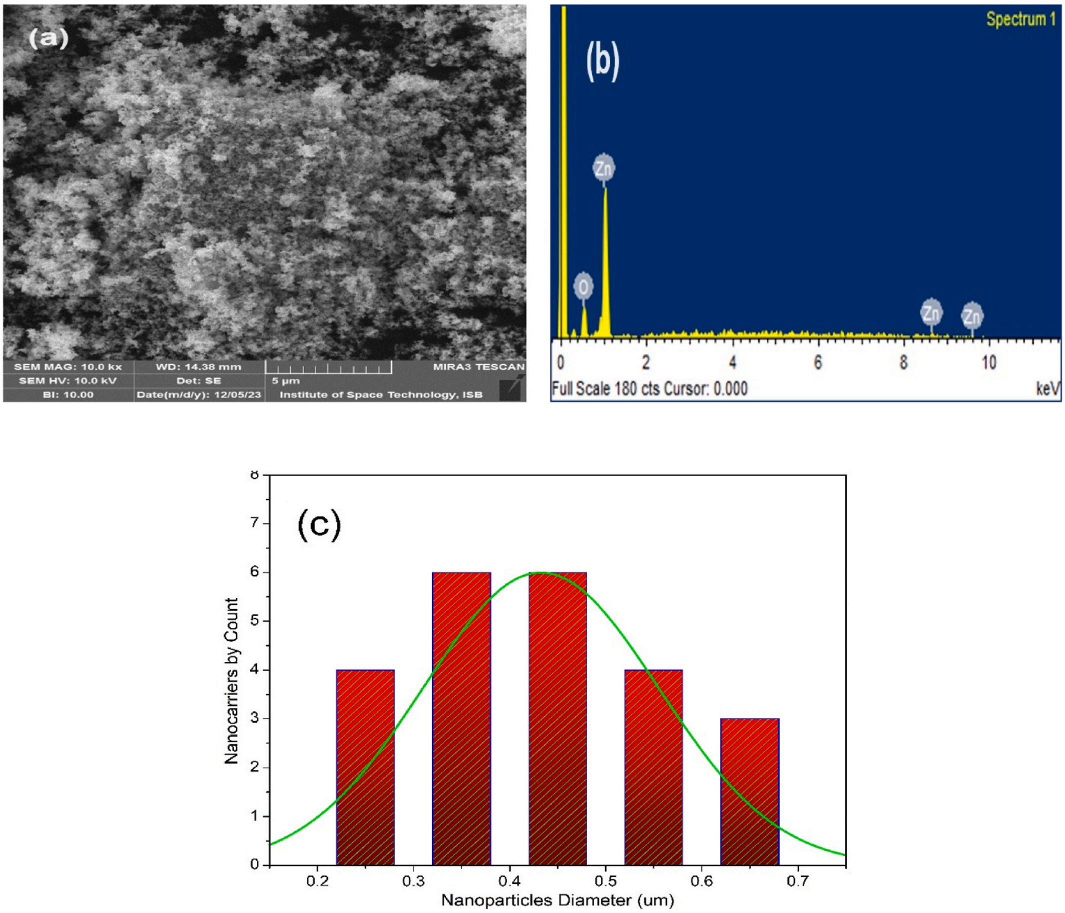

Fig. 4. (a)SEM image of ZnO (b) ZnO nanocarriers composition by EDX analysis (c) Size of ZnO nanocarriers.

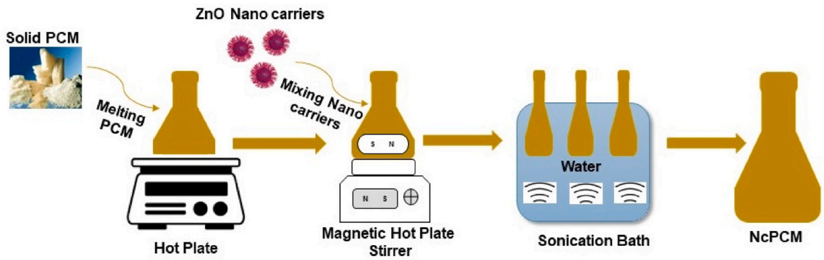

Fig. 5. Schematic description of steps involved for preparing NcPCM samples.

z = variable final value;
$z_{measured}$ = variable measured value;
δz = uncertainty in the measured variable's value as a result of instrument reading and scale fluctuations

The experimental results z_R are dependent on several measured factors, each of which has a unique uncertainty value.

$$z_R = g(z_1, z_2, z_3, \ldots\ldots, z_n) \tag{3}$$

$$\delta z_R = \sqrt{\left(\frac{\partial f}{\partial z_1}\delta z_1\right)^2 + \left(\frac{\partial f}{\partial z_2}\delta z_2\right)^2 + \ldots + \left(\frac{\partial f}{\partial z_n}\delta z_n\right)^2} \tag{4}$$

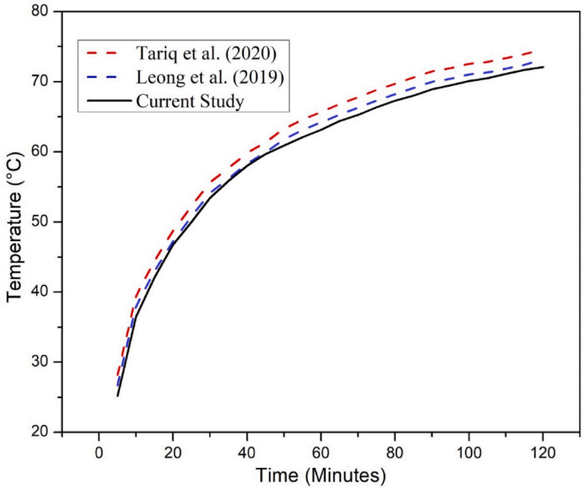

Fig. 6. Experimental Setup validation.

$$\frac{\delta z}{z_R} = \sqrt{(z_1\delta z_1)^2 + (z_2\delta z_2)^2 + \ldots + (z_n\delta z_n)^2} \tag{5}$$

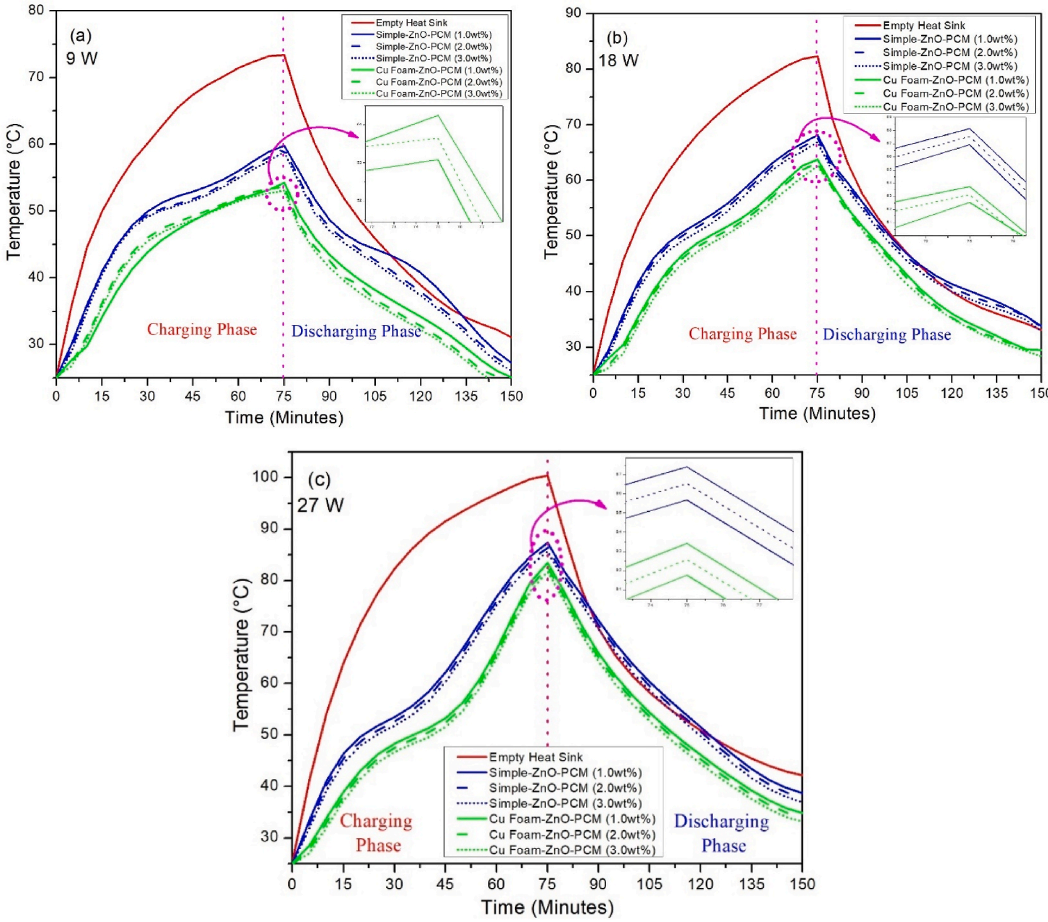

Fig. 7. Base temperature variation curves for different heat sinks with different mass fractions of ZnO based NcPCM and at heat energy of (a) 9 W (b) 18 W(c) 27 W.

$$z_n = \frac{\frac{\partial f}{\partial z_n}}{z_R} \quad (6)$$

Since the heating input uncertainty is a critical variable for the thermal evaluation of the heat sink, it is evaluated in the current scenario. The calculation of the net fractional uncertainty in the heating input involves an assessment of uncertainties associated with the applied voltage and current, along with considerations for the dimensions of the surface area, as outlined in equation (7)

$$q = g(V, I, A) \quad (7)$$

Where, $Area = f(l \times w)$

$$\frac{\partial q}{q} = \sqrt{\left[(Z_v\,\delta V)^2 + (Z_I\,\delta I)^2 + (Z_A\,\delta A)^2\right]} \quad (8)$$

$$Z_V = \frac{\frac{\partial q}{\partial V}}{q},\ Z_I = \frac{\frac{\partial q}{\partial I}}{q},\ Z_A = \frac{\frac{\partial q}{\partial A_{l,w}}}{q}$$

The uncertainties in temperature due to thermocouples calibration, voltage and current, surface area (length & width) reported to as ± 0.15 °C, ±0.02 V, ±0.02 A, 0.01 mm and 0.01 mm, respectively. The calculations indicated that the uncertainties in heat flux varied from a minimum of 3.41 % to a maximum of 5.76 %.

4. Results and discussion

4.1. The impact of ZnO nanocarriers concentration on heat sink bottom temperatures

Fig. 7(a–c) highlights the base temperature variation curves of zinc oxide NcPCM based heat sinks at different mass concentrations of ZnO nanocarriers (1.0, 2.0 & 3.0 wt%) under heat energy load conditions of 9, 18 and 27 W. The effect of heat energy on the heating and cooling phases of heat sinks is analyzed over durations of 75 min each. Thermal results of the NcPCM-composites filled heat sink geometries were contrasted with the base temperature of the empty sink (without NcPCM and foam), serving as a reference.

At 9 W heat energy, maximum temperature of unfilled heat sink at the end of heating phase reached 73.4 °C, causing a risk failure for electronics components which are commercially designed to withstand at temperatures below 70 °C at danger of malfunctioning. Hence, it's imperative to reduce the heat sink's base temperature. The sudden increase in temperature was reduced after NcPCM was inserted into heatsink cavity. Incorporating 1.0 wt% of ZnO into RT54HC led to peak temperature reductions of 18.57 % and 26.09 % for simple and foam heat sinks, respectively as shown in Fig. 7(a). This was ascribed to the excellent heat conductivity and conveying heat capabilities of ZnO nanocarriers within RT54HC. However, the temperature curves exhibit less steepness for the NcPCM configuration due to the sensible heat storage within the PCM. As fraction of ZnO nanocarriers increased into PCM from 2.0 wt% to 3.0 wt%, it effectively works in further reducing the base temperature 19.14 %–19.87 % for simple heat sink. At subjected nano-composites, maximum base temperatures showed by thermocouples were 59.34 °C and 58.80 °C. The foam composites configuration (2.0 wt% and 3.0 wt%) demonstrated the most significant temperature reduction, quantified at 26.90 % and 27.67 % respectively, compared with empty sink. The lower fraction of nanocarriers caused a small drop in base temperature but valuable improvement was observed at 3.0 wt% due to altered PCM's thermophysical characteristics. The foam-based heat sink showed optimum thermal performance.

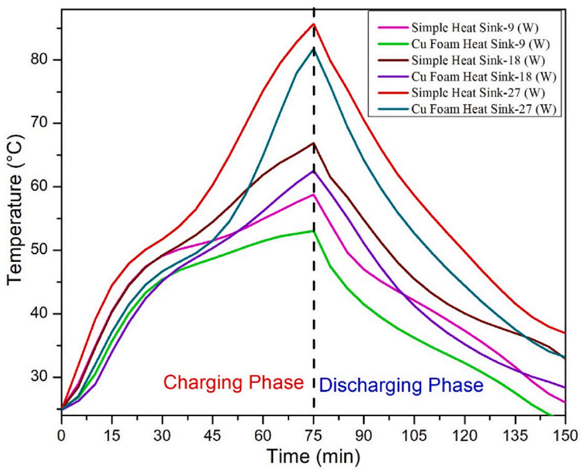

Fig. 8. Different temperatures at the bottom of the heat sink for varying heat energy (9–27 W).

Fig. 7(b) illustrates the thermal characteristics of heat sink topologies containing ZnO/RT54HC (1.0 wt%, 2.0 wt% and 3.0 wt%) under input heat energy of 18 W. The peak temperature of heat sink attained 83.30 °C without PCM/NcPCM. It reduced to 17.19 %, 17.93 % and 18.70 % respectively, as weight percentage of ZnO increases from 1.0 to 3.0. This percentage drop in temperature of PCM composites-based heat sinks at 18 W is lower compared to the values at 9 W because the higher heat energy leads to complete melting of the PCM, followed by the onset of post-sensible heating. The temperature profile of foam composites geometry showed temperatures of 63.75 °C, 63.12 °C and 62.53 °C as ZnO concentrations increases from 1.0 wt% to 3.0 wt%. At 18 W of heat energy, the peak temperature reduction percentage of metallic foam heat sink was 22.54 %, 23.31 % and 24.02 % respectively. It is concluded that the percentage reduction in peak temperature correlates with the improvement in thermal conductivity resulting from the RT54HC and ZnO blend. The incorporation of ZnO improved the thermal properties of the RT54HC, thereby enhancing the heat transfer rate.

The charging and discharging behavior of ZnO/RT54HC integrated into various heat sinks under a heating energy 27 W with 1.0 wt % to 3.0 wt% ZnO nanocarriers is shown in Fig. 7(c). The insertion of 1.0 wt% to 3.0 wt% of ZnO into PCM resulted in reduction of peak temperatures of simple heat sinks i.e 12.92 %, 13.78 % and 14.63 %, respectively. The swift melting of PCM composites causes a build-up of nanocarriers at the base, which lowers the proportion of base temperature as compared to applied heat energy of 18 W. Under the applied heat energy and using ZnO nanocarriers as a heat transfer medium in a foam sink proved to be effective. The maximum reduction in temperature for foam heat sink was observed 16.89 %, 17.72 % and 18.53 %, respectively, as nanocarriers concentration varies 1.0 wt% to 3.0 wt% into RT54HC.

To facilitate thermal analysis, Fig. 8 shows the base temperature time profiles of simple and foam heat sinks under varied heating energy and higher ZnO concentrations (3.0 wt%) in RT-54HC during the charging and discharging stages. At 9 W–27 W, foam heat sink showed efficient thermal performance as compared to simple heat sinks. At lower heat energy 9 W, The NcPCM did not undergo phase change until the end of charging phase for foam heat sink. This is made possible by the cooling media's substantial heat-absorbing capability and wide surface area for heat transfer of foam.

4.2. Critical temperature analysis to monitor heat sink thermal performance

The maximum temperature at which different portable electrical gadgets may operate varies based on their design. When these

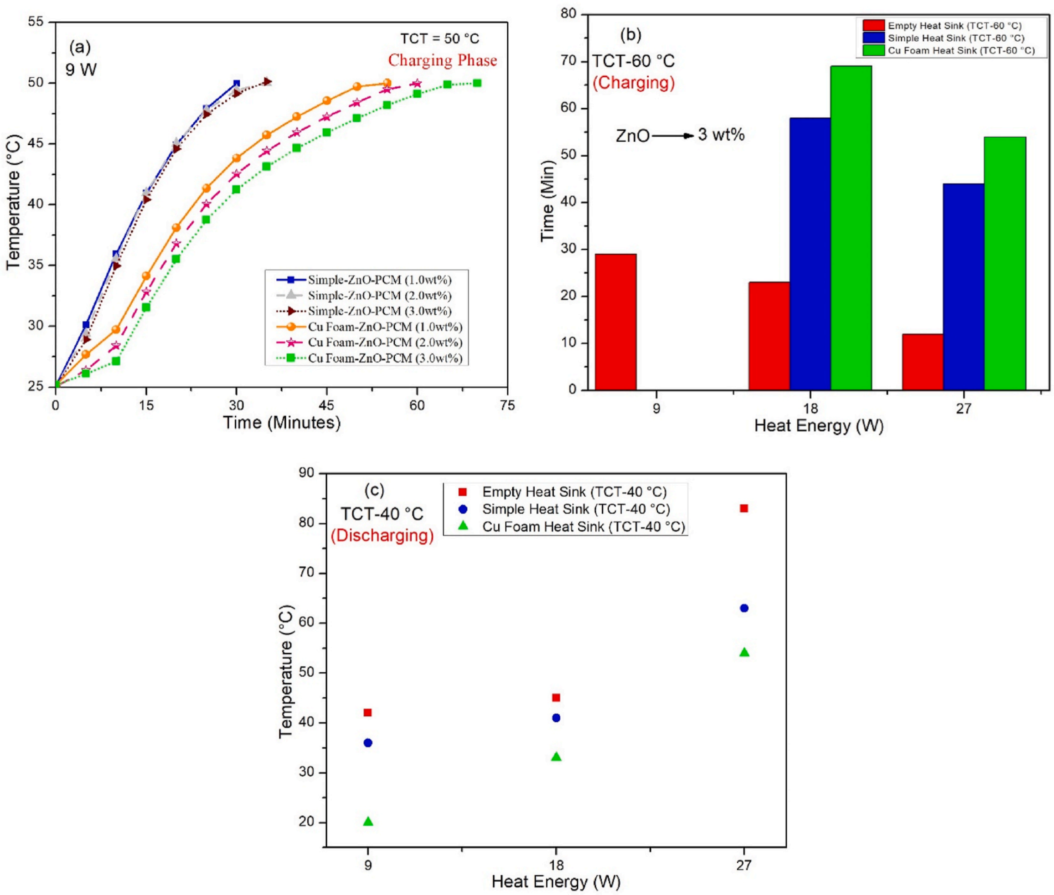

Fig. 9. Various heat sinks performance at TCTs (a) 50 °C during charging at 9 W (b) 60 °C during charging (c) 40 °C during discharging.

specified temperature thresholds are exceeded, the integrated chips in these devices may become less dependable and durable, resulting in the loss of efficiency. To assess the thermal performance of different heat sink topologies over time, two targeted critical temperatures (TCT) are considered: 50 °C and 60 °C, which are regarded as the maximum operating temperatures for charging phase. To see notable differences in the data, one TCT (50 °C) is chosen before the melting point of RT-54HC, and the other (60 °C) is chosen after the melting point. The temperature of 40 °C is selected to monitor cooling performance of the heat sink.

In order to determine which heat sink performs best, Fig. 9(a and b) shows how several heat sinks' operating durations improve at TCT of 50 °C. The lack of an isothermal heat storage medium allowed the reference empty heat sink to reach TCT fast. It is evident from Fig. 9(a) that simple heat sink reached the TCT in 30, 34 and 35 min when ZnO nanocarriers concentration varies in heat storage medium from 1.0 wt% to 3.0 wt% at heat energy of 9 W. Likewise, foam heat sink provided TCT durations in 51, 55 and more than 69 min, respectively. The combination of excellent thermal conductivity, a large surface area for heat transfer, and a large heat storage capacity made the foam heat sink perform significantly.

Fig. 9(b) shows TCT of 60 °C to evaluate the performance of simple and Cu foam heat sinks at 3.0 wt% of ZnO nanocarriers composites and heat energy of 9–27 W. The empty reference heat sink took 29, 23 and 12 min when heat energy increased from 9 to 27 W. The simple and copper foam-based heat sinks took longer than expected to obtain the necessary TCT during charging phase. A similar trend was observed at heat energy of 18 W. At highest applied heat energy, unfilled reference sink, simple and foam-based heat sink with ZnO/RT-54HC took 12, 44 and 54 min, respectively. Foam heat sink's increased surface area for energy transfer, effective thermal conductivity, and heat capacity allowed it to perform better thermally than a standard heat sink for electronics thermal management.

The powerful thermal cooling performance of any heat sink is demonstrated by how quickly its bottom temperature may be lowered. Fig. 9(c) illustrates the cooling performance comparison between simple and foam heat sinks employing NcPCM during the discharging phase of a PCM containing 3.0 wt% of nanocarriers in RT54HC, under specified heating energy loads. At 9 W, these heat sinks took 37 and 15 min, respectively, to reach TCT of 40 °C. Likewise, at 20 W, foam heat sink demonstrates the highest cooling capacity in effectively dispersing heat to the surroundings, whereas simple heat sink exhibits the lowest performance in this regard. The foam and simple sinks took 49 and 63 min to attain TCT of 40 °C.

4.3. Effect of ZnO nanocarriers and heat energy on absolute temperature and operational duration increment

Table 3 presents the % absolute temperature fall (ATF) alongside operational duration increment (ODI) of heat sink configurations at TCT of 50 °C for various concentrations of ZnO and different heat energy loads. Equations (9) and (10) offer a method to calculate ATF and ODI.

$$\%\ \text{Absolute temperature fall} = \frac{\left[\left(T_{\text{Peak:empty Sink}}\right) - \left(T_{\text{Peak Sink}}\right)\right]*100}{T_{\text{Peak:empty HS}}} \tag{9}$$

$$\text{Operational Duration Increment (ODI)} = \left[\left(\text{Time}_{\text{TCT}-50:\text{Sink}}\right) - \left(\text{Time}_{\text{TCT}-50:\text{Empty sink}}\right)\right] \tag{10}$$

Due to the heat sink experiencing high heat penetration, the ATF dropped as the heat energy loads rose. As the concentration of nanocarriers grew from 1.0 wt% to 3.0 wt%, the %ATF of the simple heat sink increased from 18.57 to 19.87 for 9W. The heat sink bottom temperature has decreased, which is the cause of this increase in ATF. Nevertheless, the period of OTE escalation extended from 15 to 19.20 min. Under all heat energy loads, similar trends were seen in different heat sink arrangements. For heat energy of 27 W and a nanocarrier concentration of 3.0 wt%, the ATF values for simple and copper foam heat sinks were recorded as 14.63 % and 18.53 %, respectively. Correspondingly, the ODI durations were 15.50 and 29.50 min, respectively. The exemplary thermal performance of heat sink having copper foam with a 3.0 wt% concentration of nanocarriers is depicted in Fig. 10, demonstrating its superior effectiveness in managing heating loads linked to electronic devices.

4.4. Comparison of results with thermal conductivity improvement methods

The literature provides a comprehensive analysis of methods aimed at improving thermal conductivity in electronic devices. This includes the integration of PCMs with various extended surface configurations in heat sinks, the incorporation of nanocarriers with

Table 3
The comparison between % decrease in absolute temperature and operating time.

ZnO fraction in PCM (wt.%)	Absolute Temp. Decrease & Operational Duration Improvement (%, min)	Heat Energy (9 W)		Heat Energy (18 W)		Heat Energy (27 W)	
		Simple Heat Sink	Cu Foam Heat Sink	Simple Heat Sink	Cu Foam Heat Sink	Simple Heat Sink	Cu Foam Heat Sink
1.0	ATF	18.57	26.09	17.19	22.54	12.92	16.89
	ODI	15	37.80	14.20	26.80	12.90	26.30
2.0	ATF	19.14	26.90	17.93	23.31	13.78	17.72
	ODI	18.10	42.80	17.30	29.30	14.80	28.40
3.0	ATF	19.87	27.67	18.70	24.02	14.63	18.53
	ODI	19.20	45.80	18.70	31.30	15.50	29.50

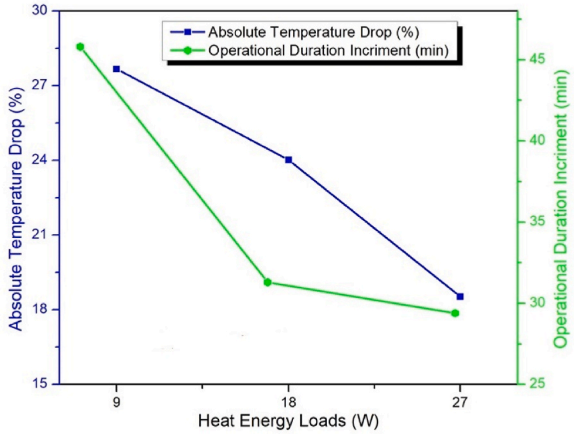

Fig. 10. Comparative analysis of the Cu foam heat sink's absolute temperature drop and operational duration increment at 3.0 wt of ZnO.

PCMs across different heat sink designs, and the application of metallic foams within heat sinks. This study investigates the thermal regulation of heat sinks through the integration of ZnO nanocarriers into PCM, focusing on both simple and foam-based heat sink designs. The objective of this study is to reduce the base temperature of the heat sink while improving the operational duration within optimal thermal conditions. The results of current and previous studies [23,41,47,57–60] using various thermal conductivity improvements methods are discussed in Fig. 11. The application of PCM in conjunction with different fin configurations in heat sink design contributes to a reduction in base temperature. Arshad et al. [58] used square pin fin of different thickness as thermal conductivity enhancer and improved operating time of device. Rehman et al. [41] used copper and nickel foam as thermal conductivity enhancer of the PCM and reduced base temperature 14.5 % and 17 %, respectively. However, the integration of nano-PCM results in a more significant decrease in base temperature, thereby enhancing the operational duration of the device. But, the nano-PCM significantly reduced the base temperature due to its enhanced surface area, while the addition of metallic foam which contributed to remove more heat from the hot temperature system to low temperature reservoir.

5. Conclusion

An experimental examination was conducted to optimize simple and foam-based heat sinks using ZnO nanocomposites integrated with PCM for improved environmental sustainability. This analysis aimed to assess their effectiveness for passive thermal management for portable electronics employing diverse heat energy loads. The influence of nanocarriers (ZnO) at optimal concentrations (1 wt% to 3 wt%) within RT54HC, along with varying heat energy loads, was analyzed in relation to the base temperatures of heat sink topologies and their operational critical temperatures. These results were compared with an unfilled reference simple heat sink to achieve optimal thermal management performance. The continuous high temperature profile of the simple empty sink, under all imposed thermal loads, may adversely affect electronic components. The integration of ZnO-reinforced RT54HC enhanced the performance of all heat sinks examined at lower temperatures. Out of all of them, the simple sink exhibited the least efficacy in bringing down the device's bottom temperature and increasing its device operational lifespan. The foam-based heat sink demonstrated enhanced optimal performance relative to the conventional sink, owing to its augmented effective surface area provided by the integration of high-porosity foam, which facilitated improved heat dissipation and thermal regulation. Overall, the copper foam sink- RT54HC excelled other conventional sink with all mass concentrations of ZnO in terms of thermal performance throughout the heating aspects enabling it to successfully reach the targeted critical temperatures of 50 °C and 60 °C. ZnO nanocarriers have a smaller environmental impact due to their abundance and lack of toxicity. The utilization of active cooling systems is lessened, leading to lower energy consumption and carbon gas emissions, due to combination of ZnO and PCM. This study also suggests the integration of both active and passive cooling methodologies with highly conductive metallic foam and nanocarriers composites with cooling media.

CRediT authorship contribution statement

Muhammad Farooq: Writing – review & editing, Writing – original draft, Supervision, Project administration, Methodology, Investigation, Formal analysis, Conceptualization. **Imran Zahid:** Writing – review & editing, Investigation, Formal analysis, Data curation. **M. Yasar Javaid:** Resources, Validation, Writing – review & editing. **Noreen Sher Akbar:** Writing – review & editing, Visualization, Validation, Software. **Enio Pedone Bandarra Filho:** Writing – review & editing, Methodology, Investigation. **M. Farrukh Shahzad:** Investigation, Visualization, Writing – review & editing. **M. Imran Khan:** Writing – review & editing, Visualization, Validation, Software. **Mohammad Ilyas Khan:** Funding acquisition, Investigation, Visualization, Writing – review & editing. **Mohammad Rehan:** Project administration, Supervision, Writing – review & editing. **Fahid Riaz:** Data curation, Funding acquisition, Resources, Writing – review & editing.

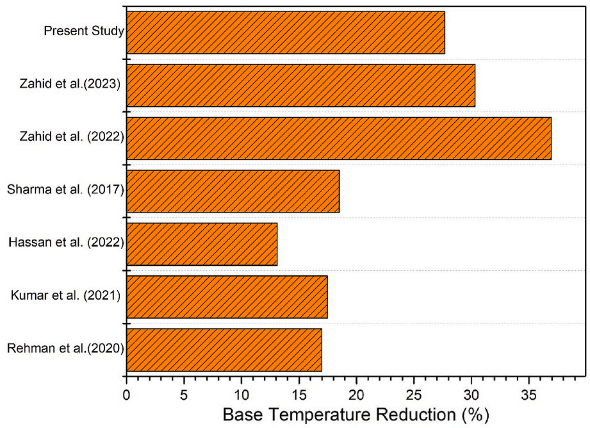

Fig. 11. Comparison of thermal management performance: Present study vs previous studies [23,41,47,49,59,60].

Declaration of competing interest

I on the behalf of the all authors, declare that there is no conflict of interest and all the elements of the submission are also in compliance with the journal publishing ethics. By submitting this manuscript, the authors agreed that the copyright for their article should be transferred to this journal if the article is accepted for publication. The work contained within the research paper is our original contribution and has not been published anywhere.

Acknowledgments

The authors extend their appreciation to the Deanship of Research and Graduate Studies at King Khalid University for funding this work through Large Research Project under grant number RGP2/533/45.

Data availability

Data will be made available on request.

References

[1] J. Xu, C. Zhang, Z. Wan, X. Chen, S.H. Chan, Z. Tu, Progress and perspectives of integrated thermal management systems in pem fuel cell vehicles: a review, Renew. Sustain. Energy Rev. 155 (2022) 111908, https://doi.org/10.1016/j.rser.2021.111908.
[2] W. Zeng, Y. Niu, S. Li, S. Hu, B. Mao, Y. Zhang, Cooling performance and optimization of a new hybrid thermal management system of cylindrical battery, Appl. Therm. Eng. 217 (2022) 119171, https://doi.org/10.1016/j.applthermaleng.2022.119171.
[3] G. Qu, Z. Deng, W. Guo, Z. Peng, Q. Jia, E. Deng, H. Zhang, The heat-dissipation sintered interface of power chip and heat sink and its high-temperature thermal analysis, IEEE Trans. Compon. Packag. Manuf. Technol. 13 (6) (2023) 816–822, https://doi.org/10.1109/TCPMT.2023.3290303.
[4] J. Zhang, D. Shao, L. Jiang, G. Zhang, H. Wu, R. Day, W. Jiang, Advanced thermal management system driven by phase change materials for power lithium-ion batteries: a review, Renew. Sustain. Energy Rev. 159 (2022) 112207, https://doi.org/10.1016/j.rser.2022.112207.
[5] M. Huang, L. Wang, C. Wang, Y. Li, J. Wang, J. Yuan, W. Xu, Optimizing crack initiation energy in austenitic steel via controlled martensitic transformation, J. Mater. Sci. Technol. 198 (2024) 231–242, https://doi.org/10.1016/j.jmst.2024.02.019.
[6] X. Pu, Z. Zhao, M. Sun, Y. Huang, Numerical study on temperature distribution uniformity and cooling performance of manifold microchannel heat sink, Appl. Therm. Eng. 237 (2024) 121779, https://doi.org/10.1016/j.applthermaleng.2023.121779.
[7] F. Hadi, H.M. Ali, Z. Khattak, M.M. Janjua, An evaluation of heat transfer and pressure drop performance of superhydrophobic surfaced integral mini-channel heat sinks with nanofluids, J. Therm. Anal. Calorim. 149 (4) (2024) 1515–1533, https://doi.org/10.1007/s10973-023-12735-8.
[8] I. Afaynou, H. Faraji, K. Choukairy, A. Arshad, M. Arıcı, Heat transfer enhancement of phase-change materials (PCMs) based thermal management systems for electronic components: a review of recent advances, Int. Commun. Heat Mass Tran. 143 (2023) 106690, https://doi.org/10.1016/j.icheatmasstransfer.2023.106690.
[9] J. Sun, Z. Zhang, Y. Zhang, X. Zhang, J. Guo, Q. Fu, L. Wu, High-temperature ablation resistance prediction of ceramic coatings using machine learning, J. Am. Ceram. Soc. 108 (1) (2025) e20136, https://doi.org/10.1111/jace.20136.
[10] H.-C. Chiu, M.-J. Youh, R.-H. Hsieh, J.-H. Jang, B. Kumar, Numerical investigation on the temperature uniformity of micro-pin-fin heat sinks with variable density arrangement, Case Stud. Therm. Eng. 44 (2023) 102853, https://doi.org/10.1016/j.csite.2023.102853.
[11] T. Rehman, U. Sajjad, B. Lamrani, A. Shahsavar, H.M. Ali, W.-M. Yan, C.W. Park, Investigation on the thermal control and performance of PCM–porous media-integrated heat sink systems: deep neural network modelling employing experimental correlations, Renew. Energy 220 (2024) 119719, https://doi.org/10.1016/j.renene.2023.119719.
[12] T. Rehman, C. Woo Park, Optimising heat sink performance with porous media–PCM integration: an experimental investigation, Appl. Therm. Eng. 242 (2024) 122506, https://doi.org/10.1016/j.applthermaleng.2024.122506.
[13] B. Hadidi, F. Veysi, R. Ghasemi, Experimental investigation of the effects of using PCM, multi-PCMs, and forced convection on heat sinks for thermal management of electronic devices, J. Therm. Anal. Calorim. 148 (14) (2023) 7441–7462, https://doi.org/10.1007/s10973-023-12232-y.
[14] C. Ma, J. Hu, M. Li, X. Deng, J. Yang, J. He, S. Weng, Multi-objective topology optimization for cooling element of precision gear grinding machine tool, Int. Commun. Heat Mass Tran. 160 (2025) 108356, https://doi.org/10.1016/j.icheatmasstransfer.2024.108356.
[15] M.T. Tahir, S. Anwar, N. Ahmad, M. Sattar, U.W. Qazi, U. Ghafoor, M.R. Bhutta, Thermal management of microelectronic devices using nanofluid with metal foam heat sink, Micromachines 14 (7) (2023) 1475, https://doi.org/10.3390/mi14071475.

[16] A. Tiwari, A.K. Patil, M. Kumar, Geometrical effects of pins in a center cleared heat sink on thermal management of electronic systems, Numer. Heat Tran., Part A: Applications 0 (0) (2023) 1–16, https://doi.org/10.1080/10407782.2023.2210257.
[17] B.K. Choure, T. Alam, R. Kumar, A review on heat transfer enhancement techniques for PCM based thermal energy storage system, J. Energy Storage 72 (2023) 108161, https://doi.org/10.1016/j.est.2023.108161.
[18] R.K. Rajamony, J.K.S. Paw, J. Pasupuleti, A.K. Pandey, C.T. Yaw, S.K. Tiong, T. Yusaf, M. Samykano, A.G.N. Sofiah, I.A. Laghari, O.A. Ahmed, K. Kadirgama, Experimental investigation on the performance of binary carbon-based nano-enhanced inorganic phase change materials for thermal energy storage applications, J. Energy Storage 86 (2024) 111373, https://doi.org/10.1016/j.est.2024.111373.
[19] H. Behi, D. Karimi, R. Youssef, M. Suresh Patil, J. Van Mierlo, M. Berecibar, Comprehensive passive thermal management systems for electric vehicles, Energies 14 (13) (2021) 3881, https://doi.org/10.3390/en14133881.
[20] J. Shafi, M. Sheremet, M. Fteiti, A.M. Saeed, M. Ghalambaz, Computational study of phase change heat transfer and latent heat energy storage for thermal management of electronic components using neural networks, Mathematics 11 (2) (2023) 356, https://doi.org/10.3390/math11020356.
[21] I. Zahid, M. Farooq, M. Farhan, Phase change materials (PCMs), in: Z. Said, A.K. Pandey (Eds.), Nano Enhanced Phase Change Materials, Springer Nature Singapore, Singapore, 2023, pp. 11–44, https://doi.org/10.1007/978-981-99-5475-9_2.
[22] Y. Zhou, R. Duan, Leak-proof reversible thermochromic microcapsule phase change materials with high latent thermal storage for thermal management, ACS Appl. Energy Mater. 7 (14) (2024) 5944–5956, https://doi.org/10.1021/acsaem.4c01282.
[23] F. Hassan, A. Hussain, F. Jamil, A. Arshad, H.M. Ali, Passive cooling analysis of an electronic chipset using nanoparticles and metal-foam composite PCM: an experimental study, Energies 15 (22) (2022) 8746, https://doi.org/10.3390/en15228746.
[24] A.K. Thakur, M.S. Ahmed, H. Kang, R. Prabakaran, Z. Said, S. Rahman, R. Sathyamurthy, J. Kim, J.-Y. Hwang, Critical review on internal and external battery thermal management systems for fast charging applications, Adv. Energy Mater. 13 (11) (2023) 2202944, https://doi.org/10.1002/aenm.202202944.
[25] J. Ranjbar Kermani, M. Mahlouji Taheri, H. Pakzad, M. Minaei, M.A. Bijarchi, A. Moosavi, M.B. Shafii, Hybrid battery thermal management systems based on phase transition processes: a comprehensive review, J. Energy Storage 86 (2024) 111227, https://doi.org/10.1016/j.est.2024.111227.
[26] G. Marseglia, M.G. De Giorgi, P. Pontes, R. Solipa, R.R. Souza, A.L.N. Moreira, A.S. Moita, Enhancement of microchannel heat sink heat transfer: comparison between different heat transfer enhancement strategies, Exp. Therm. Fluid Sci. 150 (2024) 111052, https://doi.org/10.1016/j.expthermflusci.2023.111052.
[27] A. Nirwan, D. Gupta, R. Matta, R. Kumar, B. Mondal, Evaluation of heat transfer performance of PCM based composites for thermal management of electronics, Mater. Today: Proc. 57 (2022) 954–957, https://doi.org/10.1016/j.matpr.2022.03.234.
[28] Y. Su, J. Zhu, X. Long, L. Zhao, C. Chen, C. Liu, Statistical effects of pore features on mechanical properties and fracture behaviors of heterogeneous random porous materials by phase-field modeling, Int. J. Solid Struct. 264 (2023) 112098, https://doi.org/10.1016/j.ijsolstr.2022.112098.
[29] V. Bianco, M. De Rosa, K. Vafai, Phase-change materials for thermal management of electronic devices, Appl. Therm. Eng. 214 (2022) 118839, https://doi.org/10.1016/j.applthermaleng.2022.118839.
[30] S.A.B. Al-Omari, Z.A. Qureshi, F. Mahmoud, E. Elnajjar, Thermal management characteristics of a counter-intuitive finned heat sink incorporating detached fins impregnated with a high thermal conductivity-low melting point PCM, Int. J. Therm. Sci. 175 (2022) 107396, https://doi.org/10.1016/j.ijthermalsci.2021.107396.
[31] O. Oyewola, A. Awonusi, O. Ismail, Performance improvement of air-cooled battery thermal management system using sink of different pin-fin shapes, Emerg. Sci. J. 6 (2022) 851–865, https://doi.org/10.28991/ESJ-2022-06-04-013.
[32] P. Michael Joseph Stalin, K.S. Prasad, K.P. Kumar, G. Hemadri, M. Rajesh, K.P. Kumar, Performance improvement of solar PV through the thermal management using a nano-PCM, Mater. Today: Proc. 50 (2022) 1553–1558, https://doi.org/10.1016/j.matpr.2021.09.111.
[33] M.O. Hamdan, S. Sakhi, A review on micro-encapsulated phase change materials (EPCM) used for thermal management and energy storage systems: fundamentals, materials, synthesis and applications, J. Energy Storage 72 (2023) 108472, https://doi.org/10.1016/j.est.2023.108472.
[34] M.S. Nedumaran, N. Gnanasekaran, K. Hooman, Extensive analysis of PCM-based heat sink with different fin arrangements under varying load conditions and variable aspect ratio, J. Energy Storage 73 (2023) 108870, https://doi.org/10.1016/j.est.2023.108870.
[35] M.Y. Tharwan, H.M. Hadidi, Experimental investigation on the thermal performance of a heat sink filled with PCM, Alex. Eng. J. 61 (9) (2022) 7045–7054, https://doi.org/10.1016/j.aej.2021.12.045.
[36] A.M. Elshaer, A.M.A. Soliman, M. Kassab, A.A. Hawwash, Boosting the thermal management performance of a PCM-based module using novel metallic pin fin geometries: numerical study, Sci. Rep. 13 (1) (2023) 10955, https://doi.org/10.1038/s41598-023-37639-3.
[37] V. Talele, P. Zhao, Effect of nano-enhanced phase change material on the thermal management of a 18650 NMC battery pack, J. Energy Storage 64 (2023) 107068, https://doi.org/10.1016/j.est.2023.107068.
[38] Y.A. Bhutto, A.K. Pandey, R. Saidur, K. Sharma, V.V. Tyagi, Critical insights and recent updates on passive battery thermal management system integrated with nano-enhanced phase change materials, Mater. Today Sustain. 23 (2023) 100443, https://doi.org/10.1016/j.mtsust.2023.100443.
[39] A. Moaveni, M. Siavashi, S. Mousavi, Passive and hybrid battery thermal management system by cooling flow control, employing nano-PCM, fins, and metal foam, Energy 288 (2024) 129809, https://doi.org/10.1016/j.energy.2023.129809.
[40] S. Saeedipour, A. Gharehghani, J. Ahbabi Saray, A.M. Andwari, M. Mikulski, Proposing a hybrid thermal management system based on phase change material/metal foam for lithium-ion batteries, World Electric. Vehicle J. 14 (9) (2023) 240, https://doi.org/10.3390/wevj14090240.
[41] T.- Rehman, H.M. Ali, Thermal performance analysis of metallic foam-based heat sinks embedded with RT-54HC paraffin: an experimental investigation for electronic cooling, J. Therm. Anal. Calorim. 140 (3) (2020) 979–990, https://doi.org/10.1007/s10973-019-08961-8.
[42] F. Jamil, M. Khiadani, H.M. Ali, M.A. Nasir, S. Shoeibi, Thermal regulation of photovoltaics using various nano-enhanced phase change materials: an experimental study, J. Clean. Prod. 414 (2023) 137663, https://doi.org/10.1016/j.jclepro.2023.137663.
[43] J. Paul, M. Samykano, A.K. Pandey, K. Kadirgama, V.V. Tyagi, Nano engineered paraffin-based phase change material for building thermal management, Buildings 13 (4) (2023) 900, https://doi.org/10.3390/buildings13040900.
[44] R. Balakrishnan, K. Govindaraj, A. Mahalingam, Y. Devarajan, Analysis of the thermal management of electronic equipment by employing silicon carbide nano-pcm-based heat sink, Environ. Sci. Pollut. Res. (2023), https://doi.org/10.1007/s11356-023-27468-2.
[45] H. Fayyaz, A. Hussain, I. Ali, H. Shahid, H.M. Ali, Experimental analysis of nano-enhanced phase-change material with different configurations of heat sinks, Materials 15 (22) (2022) 8244, https://doi.org/10.3390/ma15228244.
[46] A. Motevali, M. Hasandust Rostami, G. Najafi, W.-M. Yan, Evaluation and improvement of PCM melting in double tube heat exchangers using different combinations of nanoparticles and PCM (the case of renewable energy systems), Sustainability 13 (19) (2021) 10675, https://doi.org/10.3390/su131910675.
[47] I. Zahid, M. Farooq, I. Anwer, M. Farhan, M.Y. Javaid, M.R. Lashari, M. Sultan, A.U. Rehman, M. Abbas Naqvi, Q. Ali, J.M. Andresen, Experimental investigation for thermal performance of various heat sinks by alumina RT-70HC (NsPCM): sustainable approach for thermal energy storage applications, Int. Commun. Heat Mass Tran. 149 (2023) 107091, https://doi.org/10.1016/j.icheatmasstransfer.2023.107091.
[48] I. Zahid, A. Qamar, M. Farooq, F. Riaz, M.S. Habib, M. Farhan, M. Sultan, A.U. Rehman, M.A. Hayat, Experimental optimization of various heat sinks using passive thermal management system, Case Stud. Therm. Eng. 49 (2023) 103262, https://doi.org/10.1016/j.csite.2023.103262.
[49] I. Zahid, M. Farooq, M. Farhan, M. Usman, A. Qamar, M. Imran, M.A. Alqahtani, S. Anwar, M. Sultan, M.Y. Javaid, Thermal performance analysis of various heat sinks based on alumina NePCM for passive cooling of electronic components: an experimental study, Energies 15 (22) (2022) 8416.
[50] I. Zahid, M. Farhan, M. Farooq, M. Asim, M. Imran, Experimental investigation for thermal performance enhancement of various heat sinks using Al2O3 NePCM for cooling of electronic devices, Case Stud. Therm. Eng. 41 (2023) 102553.
[51] C. Yadav, R.R. Sahoo, Thermal analysis comparison of nano-additive PCM-based engine waste heat recovery thermal storage systems: an experimental study, J. Therm. Anal. Calorim. 147 (3) (2022) 2785–2802, https://doi.org/10.1007/s10973-021-10611-x.
[52] C.D. Liyanage, H. Kumar, I. Perera, P.G. Abeykoon, F. Chen, J.S. Joya, S.L. Suib, D.H. Adamson, Synthesis of graphene oxide: effect of sonication during oxidation, Carbon 223 (2024) 119047, https://doi.org/10.1016/j.carbon.2024.119047.
[53] S. Jegadheeswaran, A. Sundaramahalingam, Experimental investigations of the effect of ultrasonic waves on the thermal performance of nanoparticles embedded phase change material, Int. J. Thermophys. 44 (1) (2022) 8, https://doi.org/10.1007/s10765-022-03123-9.

[54] K.Y. Leong, S.P. Chew, B.A. Gurunathan, K.Z. Ku Ahmad, H.C. Ong, An experimental approach to investigate thermal performance of paraffin wax and 1-hexadecanol based heat sinks for cooling of electronic system, Int. Commun. Heat Mass Tran. 109 (2019) 104365, https://doi.org/10.1016/j.icheatmasstransfer.2019.104365.
[55] S.L. Tariq, H.M. Ali, M.A. Akram, M.M. Janjua, Experimental investigation on graphene based nanoparticles enhanced phase change materials (GbNePCMs) for thermal management of electronic equipment, J. Energy Storage 30 (2020) 101497, https://doi.org/10.1016/j.est.2020.101497.
[56] S.J. Kline, Describing uncertainties in single-sample experiments, Mech. Eng. 75 (1963) 3–8.
[57] T.- Rehman, T. Ambreen, H. Niyas, P. Kanti, H.M. Ali, C.-W. Park, Experimental investigation on the performance of RT-44HC-nickel foam-based heat sinks for thermal management of electronic gadgets, Int. J. Heat Mass Tran. 188 (2022) 122591, https://doi.org/10.1016/j.ijheatmasstransfer.2022.122591.
[58] A. Arshad, H.M. Ali, M. Ali, S. Manzoor, Thermal performance of phase change material (PCM) based pin-finned heat sinks for electronics devices: effect of pin thickness and PCM volume fraction, Appl. Therm. Eng. 112 (2017) 143–155, https://doi.org/10.1016/j.applthermaleng.2016.10.090.
[59] S. Sharma, L. Micheli, W. Chang, A.A. Tahir, K.S. Reddy, T.K. Mallick, Nano-enhanced phase change material for thermal management of BICPV, Appl. Energy 208 (2017) 719–733, https://doi.org/10.1016/j.apenergy.2017.09.076.
[60] A. Kumar, R. Kothari, S.K. Sahu, S.I. Kundalwal, A comparative study and optimization of phase change material based heat sinks for thermal management of electronic components, J. Energy Storage 43 (2021) 103224, https://doi.org/10.1016/j.est.2021.103224.